

Synthesis of glassy composite $As_{0.63}S_{2.70}Sb_{1.37}Te_{0.30}$ and its physical properties

MIHAI IOVU¹, VICTOR VERLAN^{1,*}, OLGA BORDIAN¹, MARIUS ENACHESCU^{2,4}, AURELIAN POPESCU^{3,*}, DAN SAVASTRU³, LAURA-BIANCA ENACHE², SABRINA ROSOIU², MATEI BARDEANU², OANA ANDREEA LAZAR², GEANINA MIHAI⁴

¹Institute of Applied Physics, Str. Academiei 5, MD-2028 Chisinau, R. Moldova

²Center for Surface Science and Nanotechnology, University Politehnică of Bucharest, Splaiul Independentei 313, 060042 Bucharest, Romania

³National Institute of Research and Development for Optoelectronics INOE 2000, Str. Atomistilor 409, 077125, Magurele, Romania

⁴S.C. NanoPRO START MC S.R.L., 110310 Pitesti, Romania

The nanostructured glassy semiconductor $As_{0.63}S_{2.70}Sb_{1.37}Te_{0.30}$ was synthesized and thin films of this material were obtained. The physical and structural properties of the bulk material and thin layers were characterized using SEM-EDX electron microscopy, XRD diffraction, and micro-Raman. Detailed investigations showed the amorphous and homogeneous nature of the samples. The average coordination number of the composite of 2.4 and the electrons lone pair of 3.2 were determined.

(Received October 28, 2022; accepted December 5, 2022)

Keywords: Chalcogenide glasses, $As_{0.63}S_{2.70}Sb_{1.37}Te_{0.30}$, XRD, Micro-Raman, SEM-EDX

1. Introduction

Chalcogenide glasses are intensively studied due to their applications in photonics, electro- and optoelectronics such as: components for application in the infrared domain, materials for image recording and holographic information storage, acousto-optical elements, optical memory switches [1-4], etc.

These materials have a low level of phonons and are considered glasses with heavy anions, since sulphur, selenium and even tellurium are the main components of their compositions. They are further studied for applications in passive and active devices such as fibre laser amplifiers and nonlinear components [3]. These chalcogenide materials possess unique properties such as photodarkening, huge photoexpansion, and photofluidity when illuminated by appropriate light [5].

Chalcogenide glasses form a wide range of compositions with homo- and heteropolar bonds. The increasing the relative atomic mass of chalcogen and the proportion of chalcogen in glasses reduces the average bond strength, increases volatility and elasticity. Their outstanding properties are: the ease of forming massive materials and thin films, excellent optical transmission in the visible and infrared region, resistance to atmospheric conditions, high chemical stability, sensitivity to light irradiation and electron beam action [6,7].

Unlike crystalline materials that present long-range structural order, described by correlations between atoms independent of their distance, non-crystalline solids are characterized only by short-range order in the 0.2 – 0.4 nm range and by interatomic correlation in the first

coordination sphere of an arbitrary atom. For amorphous materials with covalent networks, the short-range order contains local coordination pyramids such as AsS_3 and SbS_3 [6]. For covalent glasses there are also medium-intermediate distance orders, extending to the 0.5-1.0 nm range. The order of the intermediate interval has an important role in the properties of glasses [8,9].

Arsenic is a good glass former and has a good glass forming region with S , Se and Te , but its binary composites have the disadvantage for some applications: they have optical bandgap in a large energy range and optical loss occurs in the transparency band, which causes difficulties in optical communication over long distances. To eliminate such discrepancies and to improve optical properties in the infrared range, elements with higher atomic mass such as Sb and Te are added [10,11]. The partial substitution with $Sb_2(S,Te)_3$ in As_2S_3 and in the $As-S-Sb-Te$ system has a predominant character by involving the formation of a highly stable network structure with good transparency in the infrared range of the spectrum. Glassy semiconductors containing both the elements Sb and Te are also known as good "ovonic" materials for volatile memory, which have intermediate distance orders that play an important role in controlling the properties of covalent glass [12-14].

This paper presents the extension of our previous experimental results [15,16] regarding multi components chalcogenide alloys. In order to combine these two advantages of short distance and medium-intermediate distance with the increase of volatility and elasticity in a single composition, in this work an optimal vitreous composition of four elements $As_{0.63}S_{2.70}Sb_{1.37}Te_{0.30}$ was

obtained and its physical properties were analysed. The main attention is focused on the synthesis and characterization of the glassy composite $As_{0.63}S_{2.70}Sb_{1.37}Te_{0.30}$ in bulk, powder and thin layer form.

2. The experimental methods

To measure the properties of the composite $As_{0.63}S_{2.70}Sb_{1.37}Te_{0.30}$ in the form of massive material, powder and thin layers, the equipment available to the CSSNT group from the Politehnica University of Bucharest, Romania was applied.

2.1. SEM-EDX scanning electron microscopy method

Microscopic analyses were performed using the Hitachi HD-2700 SEM system, equipped with Energy Detector-X-ray dispersive analyser. For measurements, the material was dispersed in ethanol, sonicated and deposited on a standard Cu grid. SEM images were recorded at the same location on the sample using secondary electron (SE), phase contrast (PhC) and transmission electron (TE) detectors.

2.2. X-ray diffraction investigations

XRDs were performed using a SmartLab High Resolution Equipment Rigaku X Ray Diffractometer, $Cu: K_{\beta}I=1.39217 \text{ \AA}$, $K_{\alpha}I=1.540598 \text{ \AA}$ and $Cu K\alpha_2=1.544426 \text{ \AA}$, voltage = 45 kV, current = 200 mA. Diffractograms were recorded at room temperature over a wide range of 2θ angles (15-80 degrees) with a scan step of 0.6 degrees.

2.3. Raman studies

Micro-Raman of the samples from deposited layers were performed at room temperature with Confocal Micro-Raman Spectroscopy, using the LabRam HR800 system. All Raman spectra were generated by exposing the samples for 100 s to 632 nm the red excitation laser and by measuring the signal scattered by the sample to the CCD detector using a 600 lines/mm diffraction grating.

3. Samples preparation

3.1. Synthesis of glassy material

All chemicals were purchased from Aldrich Chemical Co. The glassy chalcogenide semiconductor $As_{0.63}S_{2.70}Sb_{1.37}Te_{0.30}$ was synthesized using the elements As , S , Sb , Te with a purity of (99.999%), in quartz ampoules. The precursors were weighed, loaded into the ampoules, then the vial was evacuated and vacuum sealed (10^{-5} mm Hg) and placed in the oven. The furnace

temperature was slowly raised at a rate of $1 \text{ }^{\circ}\text{C}/\text{min}$ up to $920 \text{ }^{\circ}\text{C}$. The maximum temperature of the liquid melt mixture was maintained for 12 hours along with rotation of the furnace around the perpendicular axis to obtain a homogeneous mass. Subsequently, melt quenching was applied. The ampoule was suddenly cooled by removing it from the oven to room temperature. Part of the synthesized ingot was ground into powders with a grain size of about 100 nm for microscopic measurements and obtaining thin films.

3.2. Preparation of thin films

The thin films were thermally deposited by vacuum evaporation (10^{-5} mm Hg) using a tantalum "quasi-closed" complex evaporator. In the construction of the vaporizer, a special cover with many holes is provided to ensure a uniform flow of vapours on the substrate so that a uniform film thickness can be obtained over an area of 100 cm^2 [17,18]. In addition, the VUP-4 vacuum plant was equipped with recorder and the temperature of the evaporator was maintained. The temperature control was carried out automatically with the VRT-2 temperature regulator. The films were obtained on optical glass substrates. The evaporation temperature of the $As_{0.63}S_{2.70}Sb_{1.37}Te_{0.30}$ material was constant during the evaporation which ensured the maintenance of a constant condensation rate during the evaporation period. The thickness of the deposited layer was determined by the evaporation time, and its homogeneity was regulated by the diaphragms mounted above the evaporator. The uniform distribution of the condensation thickness over the whole layer was also ensured by the variation of the distance between the substrate and the evaporator. The distance between the evaporator and the substrate was equal to 21 cm. Transparent amorphous films were obtained with thicknesses of $125 \div 1000 \text{ nm}$. The layer thickness was measured using the MII-4 interferometric microscope.

4. Experimental results and discussion

4.1. X-ray diffraction (XRD) study of the $As_{0.63}S_{2.70}Sb_{1.37}Te_{0.30}$ composite

Fig. 1 shows the XRD diffractograms for bulk (a) material and the powder (b). The appearance of broad peaks without sharp maxima confirms the amorphous nature of the material. These peaks are generated by the short-range order of the composite components in the amorphous network.

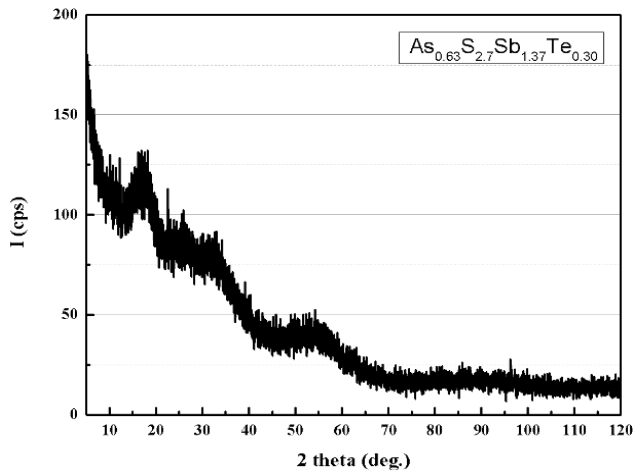


Fig. 1. XRD patterns for bulk material of $As_{0.63}S_{2.70}Sb_{1.37}Te_{0.30}$.

4.2. SEM results

The morphological and structural properties of the powder of the amorphous chalcogenide composites $As_{0.63}S_{2.70}Sb_{1.37}Te_{0.30}$ were studied by the SEM method and are presented in Fig. 2. Secondary electrons images were acquired at different magnification: 500x, x1.5K, x3K, x5K, x10K, x15K, x25K, x50K.

As can be seen, the surface morphology of the powder sample is described by the presence of particles in the form of flakes - figures, having different sizes up to 400 nm. The secondary electrons image revealed by the powder samples does not show a significant contrast variation over the investigated area.

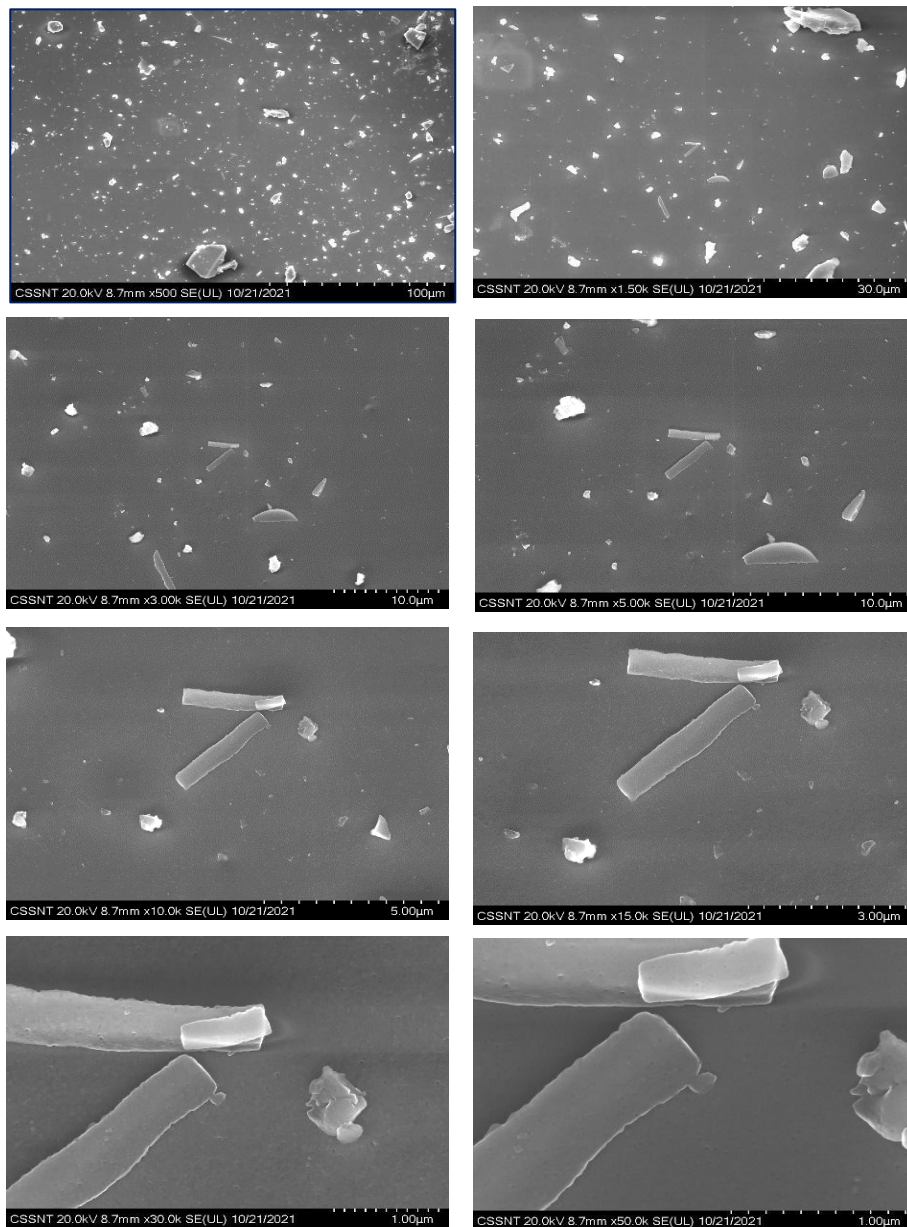


Fig. 2. Secondary electron images were obtained at various magnifications: 500x, x1.5K, x3K, x5K, x10K, x15K, x25K, x50K and x100K

4.3. Quantitative analysis and elemental distribution of the composite



The samples were analysed using Energy Dispersive X-Ray Spectroscopy (EDX) in two ways: sample area mapping and quantitative composition profile statistics on the same surface. Quantitative analysis was performed at x20K magnification. The thin film sample exhibits a smooth surface morphology (Fig. 3). Contrast variations observed in the images indicate uniform distribution of the four components (*Sb*, *As*, *S*, *Te*) in the final material. As the images of the investigated sample show, there are no observation of inhomogeneity variations. A rather uniform distribution of the elements was observed, which demonstrates the homogeneity of the material.

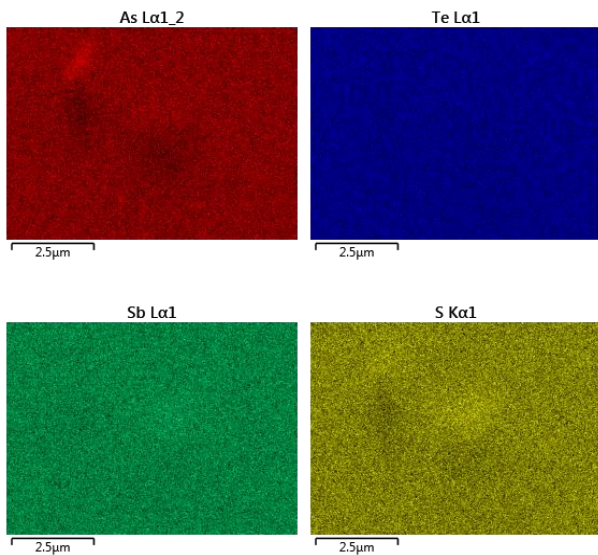


Fig. 3. The map images and the elements distribution on the same area of powder of $As_{0.63}S_{2.70}Sb_{1.37}Te_{0.30}$. Mapping was analysed at the magnification x20K (color online)

EDX analysis with quantitative statistics of the composite $As_{0.63}S_{2.70}Sb_{1.37}Te_{0.30}$ on the same surface was

performed at x20K. A good coincidence of the average measured elemental percentages of the components with the calculated one is observed (Table 1).

The measurements of the elemental composition in different places of the sample showed the same composition, which further confirms the elemental homogeneity of the sample.

Table 1. EDX statistics of the elemental composition of the composite $As_{0.63}S_{2.70}Sb_{1.37}Te_{0.30}$

Elements:	S	As	Sb	Te
Calculated, %	13.93	25.55	49.23	11.29
Average measured, %	12.73	25.05	50.06	11.72

4.4. Micro-Raman studies

The Raman spectra measurements with green laser excitation showed very low intensity, therefore all measurements were made with the red laser (632 nm).

Fig. 4 (b,d,f) illustrate the micro-Raman spectra of $As_{0.63}S_{2.70}Sb_{1.37}Te_{0.30}$ powder, thin-layer and bulk samples. Micro-Raman measurements on all sample kits revealed the presence of similar bands with small shifted deviations.

Each figure shows the measurements performed on different sample regions. Measurements were made at various points on the surface. Results are shown on the illustrated drawings. The revealed coincidence of the spectra indicates the homogeneity of the samples used for measurements. As can be seen, all investigated samples are characterized by the same main vibrational bands with very small deviations. To identify the positions of the peaks, the spectral regions were deconvoluted using the ORIGIN program with Gaussian function.

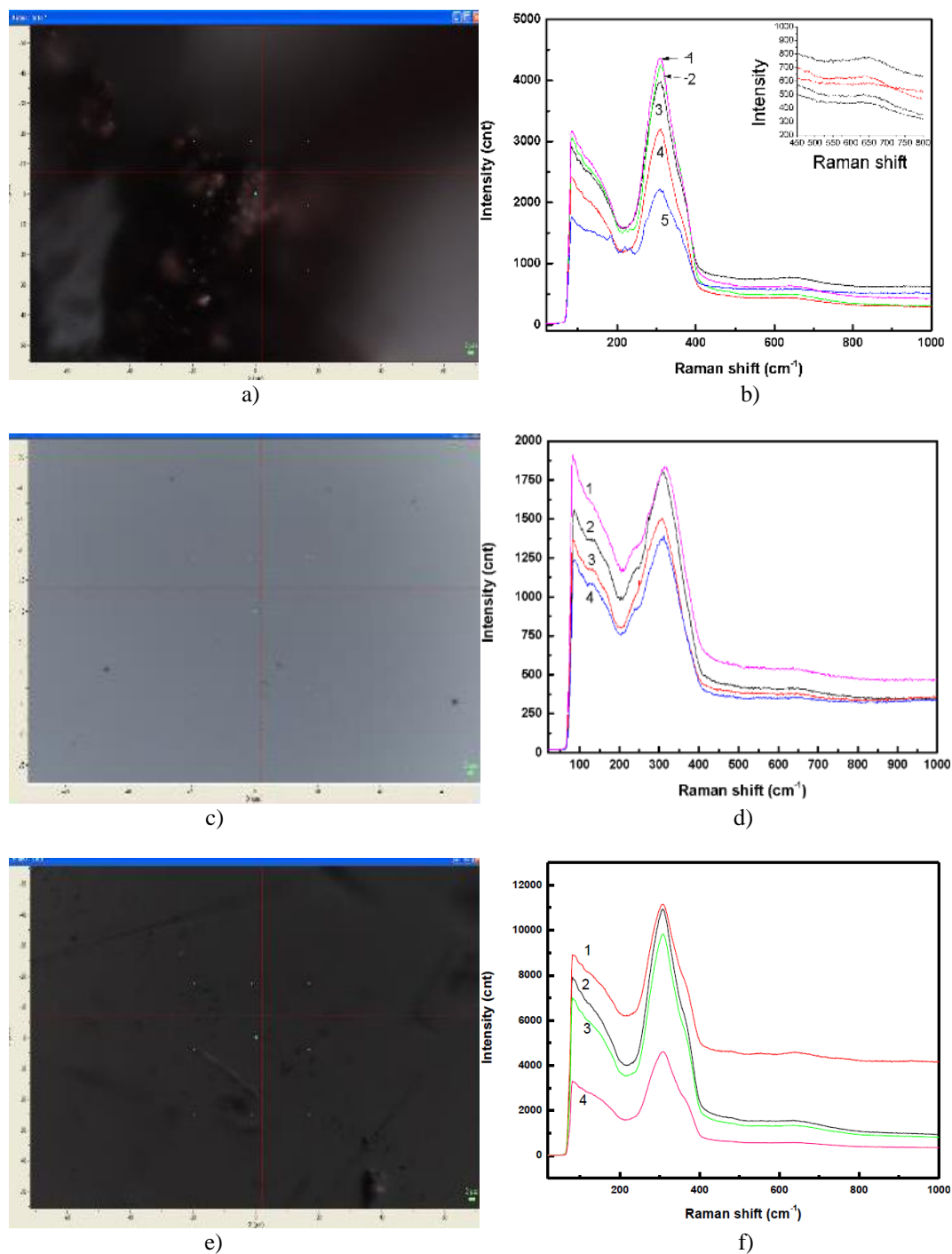


Fig. 4. Area images and Micro-Raman spectra of $As_{0.63}S_{2.70}Sb_{1.37}Te_{0.30}$ for powder (a, b), thin film (c, d) and bulk (e, f) samples. Raman spectra are shown for different analysed regions on the same sample (color online)

The positions of the maxima are given in Table 2.

The peaks can be associated with *Te-Te*, *Sb-S*, *As-As*, *Te-Te*, *Sb-Te* and *As-S* vibrations. A broad peak was observed at 310 cm^{-1} associated with *AsS3/2* and *As4S3* signal. Revealed peaks match the data known from literature [25–28].

Table 2. Maxima of micro-Raman spectra

Powder, cm^{-1}	Thin films, cm^{-1}
86,68	81,54
105,76	-
131,36	132,12
168,63	176,35
238,90	236,85
310,52	309,30
643,54	-

4.5. Average number of coordination and constraints per atom

The average coordination number N_{av} of covalent composite is a good measure representing the character of the atomic unit. The concept of average coordination number, N_{av} , is useful in describing crosslinking in a covalently bonded solid. Phillips [19], Mott [20] and Flank et al. [21] showed that the coordination number of atoms with covalent bonds in glass is determined by the 8-N rule, where N is the number of electrons in the outer electronic shell [21]. For a multicomponent alloy of the vitreous chalcogenide system, the average coordination number is defined as the average covalent coordination of the atoms in the composite. The materials in the As-Sb-S-Te system are formed by covalent bonds and the ionic character is neglected [21,22]. The pairs of atoms (*As*, *Sb*) and (*S*, *Te*) have valence electron numbers equal to 5 and 6, respectively. The 8-N rule suggests that the number of nearest neighbour atoms for (*S*, *Te*) and (*As*, *Sb*) are two and three respectively. The elements *As* and *Sb* have the atomic configuration (AC) $[Ar]3d_{10}4s_2^4p_3$ and $[Kr]4d_{10}5s_2^5p_3$ respectively and have the electronic valence (*V*) *V* = 5. The coordination number in the chemical bonds when the outer orbit is completely filled with eight electrons (8-*V*) can be *N* = 3. For sulphur AC = $[Ne]3s_2^3p_4$ and tellurium AC = $[Kr]4d_{10}5s_2^5p_4$ both have *V* = 6 and *N* = 2.

The average coordination number (N_{av}) is determined according to the formula: $N_{av} = \sum_1^4 Ni \cdot xi / \sum xi$, where N_i is the coordination number of atom *i* and x_i are the atomic weights of *As*, *Sb*, *S* and *Te* in the composite. The average coordination number (N_{av}) of the glassy composite $As_{0.63}S_{2.70}Sb_{1.37}Te_{0.30}$ determined according to this formula is equal to 2.4:

$$N_{av} = \sum_1^4 Ni \cdot xi / \sum xi = (3 \cdot 0.63 + 2 \cdot 2.70 + 3 \cdot 1.37 + 2 \cdot 0.30) / (0.63 + 2.70 + 1.37 + 0.30) = 2.4$$

which belongs to the class of semiconductor materials.

According to [23] N_{av} domains for different materials are the following: for under constrained amorphous materials 0 - 1, for semiconductor materials and glasses 2 - 3, for over constrained amorphous materials 3 - 4, for metals > 4. So, our composite with average coordination number $N_{av}=2.4$ is isostructural and this is a premise for obtaining advanced optical properties.

The number of lone pair (L) electrons for $As_{0.63}S_{2.70}Sb_{1.37}Te_{0.30}$ was calculated according to the formula [24]:

$$L = N_v - N_{av},$$

where N_v is number electrons which refers to pair of valence electrons not shared with another atom in a covalent bond. N_v was calculated using formula:

$$N_v = \sum_1^4 (8 - Ni) \cdot xi / \sum xi = (5 \cdot 0.63 + 6 \cdot 2.70 + 5 \cdot 1.37 + 6 \cdot 0.30) / (0.63 + 2.70 + 1.37 + 0.30) = 28.0 / 5 = 5.6.$$

The calculated number of lone pair electrons (L) is:

$$L = N_v - N_{av} = 5.6 - 2.4 = 3.2$$

From these results it follows that, electrons with lone pairs in the structure of the $As_{0.63}S_{2.70}Sb_{1.37}Te_{0.30}$ system have the necessary conditions to get them in a glassy state [25].

5. Conclusions

The synthesis of the glassy composite $As_{0.63}S_{2.70}Sb_{1.37}Te_{0.30}$ was done. Thin layers with same composition were obtained from bulk materials by vacuum thermal evaporation. The average coordination number per atom of 2.4 was established and the number of lone pair electrons of 3.2 was calculated. XRD, SEM and EDX investigations showed amorphous nature and homogeneous elements distribution. It is interesting that the average coordination number is the same as that of As_2S_3 , a material with high homogeneity and transparency. The material with composition $As_{0.63}S_{2.70}Sb_{1.37}Te_{0.30}$ looks to be promising as high-quality optical material.

Acknowledgment

This work was funded by ANCD Moldova through projects 20.80009.5007.14, 22 80013.5007.6BI, by European Union through projects ECSEL: H2020 MADEin4 (Ctr. no. 8/1.1.3H/06.01.2020, code POC-SMIS 128826), ECSEL -H2020 OCEAN12 (Ctr. no. 9/1.1.3H/20.01.2020, POC-SMIS code 129948), ECSEL-H2020 PIN3S (Ctr. no. 10/1.1.3H/03.04.2020, POC-SMIS code 135127), by the Romanian Ministry of Research, Innovation and Digitalization through RDI project of excellence contract 18PFE/30.12.2021, Core Program OPTRONICA PN19-18.01.01 (ctr.18N/2019) and Exploratory Research Projects Competition grant number PN-III-P4-PCE-2021-0585.

References

- [1] J. A. Savage, *J. Non-Cryst. Solids* **47**(1), 101 (1982).
- [2] A. Christy Ferdinand, M. S. Shekhawat, p. 117 in book Binder K. and Kob W., "Glassy Materials and Disordered Solids", World Scientific, Singapore (2005).
- [3] K. Binder, W. Kob, in book Binder K. and Kob W., "Glassy Materials and Disordered Solids", World Scientific, Singapore (2005).
- [4] Petronela Gheorghe, Adrian Petris, *Rom. Rep. Phys.* **74**, 404 (2022).
- [5] M. Kastner, D. Adler, H. Fritzsche, *Phys. Rev. Lett.* **37**(22), 1504 (1976).
- [6] K. N'Dri, V. Coulibaly, J. Sei, D. Houphouet-Boingny, J.-C. Jumas, *Chalcogenide Lett.* **10**(12), 533 (2013).

- [7] C. R. Schardt, J. H. Simmons, P. Lucas, L. L. Neindre, J. Lucas, *J. Non-Cryst. Solids* **274**(3), 23 (2000).
- [8] Victor K. Tikhomirov, *J. Non-Cryst. Solids* **256**, 328 (1999).
- [9] Tyler Nichol, Janis Teteris, Mara Reinfelde, Maria Mitkova, *Adv. Mat. Lett.* **10**(12), 868 (2019).
- [10] S. R. Elliott, C. N. R. Rao, J. M. Homas, *Angew. Chem. Int. Edit.* **25**, 31 (1986).
- [11] N. F. Mottand, E. A. Davis, "Electronic Process in Non-Crystalline Materials", Clarendon, Oxford, UK, (1979).
- [12] F. Sava, A. Lőrinczi, *J. Ovonic Res.* **2**(2), 4 (2006).
- [13] K. N'Dri, D. Houphouët-Boigny, G. Kra, J. C. Jumas, *CR Chim.* **10**, 498 (2007).
- [13] M. Dally, N. Kouame, D. Houphouët-Boigny, *Chalcogenide Lett.* **18**(11), 681 (2021).
- [14] R. I. Alekberov, A. I. Isayev, S. I. Mekhtiyeva, *J. Optoelectron. Adv. M.* **22**(11-12), 96 (2020).
- [15] O. Iaseniuc, M. Iovu, *Chalcogenide Lett.* **19**(2), 117 (2022).
- [16] O. V. Iaseniuc, M. Iovu, ICNBME 2021, IFMBE Proceedings **87**, 5th International Conference on Nanotechnologies and Biomedical Engineering, November 3–5, 2021, Chisinau, Moldova, 77 (2022).
- [17] A. A. Popescu, M. Mihăilescu, C. Neagu, L. Baschir, M. Stafe, G. C. Vasile, D. Savastru, M. S. Iovu, V. I. Verlan, O. T. Bordian, A. Moldovan, M. Enăchescu, N. N. Pușcaș *U.P.B. Sci. Bull. series A*: **76**(3), 1223 (2014).
- [18] A. A. Popescua, D. Savastru, L. Baschir, V. V. Verlan, O. Bordian, M. Stafe, N. Puscas, *Chalcogenide Lett.* **17**(3), 117 (2020).
- [19] J. C. Phillips, *J. Non-Cryst. Solids* **34**, 153 (1979).
- [20] N. F. Mott, *Philos. Mag.* **19**, 835 (1969).
- [21] A. M. Flank, D. Bazin, H. Dexpert, P. Lagarde, C. Mervo, J. Y. Barraud, *J. Non-Cryst. Solids* **91**, 306 (1987).
- [22] Keiji Tanaka, *Phys. Rev. B* **39**(2), 1270 (1989).
- [23] J. C. Phillips, M. F. Thorpe, *Solid State Commun.* **53**(8), 699 (1985).
- [24] S. A. Dembovskii, *Inorg. Mater. (see Izv. Akad. Nauk SSSR)* **14**, 803 (1978).
- [25] S. S. Fouad, S. A. Fayek, M. H. Ali, *Vacuum* **49**(1), 29 (1998).
- [26] Leonid Mochalov, Dominik Dorosz, Mikhail Kudryashov, Aleksey Nezhdanov, Dmitry Usanov, Daniela Gogova, Sergey Zelentsov, Aleksey Boryakov, Alexandr Mashin *Spectrochim Acta A* **193**, 258 (2018).
- [27] R. Zybala, K. Mars, A. Mikuła, J. Bogusławski, G. Soboń, J. Sotor, M. Schmidt, K. Kaszyca, M. Chmielewski, L. Ciupiński, K. Pietrzak, *Arch. Metall. Mater.* **62**(2), 1067 (2017).
- [28] K. M. F. Shahil, M. Z. Hossain, V. Goyal, A. A. Balandin, *J. Appl. Phys.* **111**(5), 054305 (2012).

*Corresponding authors: vverlan@gmail.com;
apopescu@inoe.ro